Mat. Res. Soc. Symp. Proc. Vol. 724 © 2002 Materials Research Society N7.18

Spatio-Temporal Patterns in Ferritin Crystal Growth

Olga Gliko and Peter G. Vekilov
Department of Chemical Engineering, University of Houston, Houston, TX 77204-4004

ABSTRACT

We investigate the unsteady kinetics and the formation of spatio-temporal patterns during the ferritin crystal growth, which is controlled by the rate of supply of material. For this, we apply a novel phase-shifting interferometry technique. We find that the growth rate and local slope fluctuate by up to 100% of their average values as a result of step bunching. The fluctuation amplitudes decrease with higher supersaturation and larger crystal size, as well as with increasing distance from the step sources. Since these are parameters that govern the protein supply field, we conclude that fluctuations are rooted in the coupling of the interfacial processes of growth to the bulk transport in the solution. Analysis of the step velocity dependence on local slope indicates a very weak interaction between the steps. Hence, in transport-controlled systems with non-interacting or weakly interacting steps the step bunches decay and step train tends towards its stable, equidistant state.

INTRODUCTION

The loss of stability of equidistant step trains leads to bunches of steps spreading along the crystal face, interspersed with bands of lower step density. The step bunches leave trails of higher defects density in the crystal lattice, and in this way lower the perfection and the utility of the grown crystals [1-3].

The kinetics instabilities and step bunching during the crystallization of the protein lysozyme were studied using a high-resolution interferometry technique [4]. It was concluded that fluctuations are intrinsic and result from the coupled bulk transport and interfacial kinetics processes [3]. According to this mechanism, the strongest instabilities occur when the growth proceeds under equal weights of the transport and kinetics in the overall rate control. Hence, shifts towards purely kinetic, or, conversely, purely diffusive regimes should lead to higher stability. Developed numerical model of coupled bulk transport and nonlinear interfacial kinetics quantitatively reproduces the experimentally observed unsteadiness [5]. If the rationale developed based on lysozyme data holds, in crystallization systems with dominant transport control, such as ferritin, a shift of the working point toward slower transport should dampen the fluctuations. Thus, the aim of this work is to experimentally study the origin of kinetics unsteadiness in ferritin growth. We investigate the dependencies of the amplitude of local slope fluctuations on the parameters affecting transport to the interface: supersaturation, crystal size and location on the crystal faces.

EXPERIMENTAL PROCEDURES

The crystallizing solution contains between 2–2.5 mg/mL horse spleen ferritin purchased form Sigma and purified to reduce the level of the most common impurity, the covalent dimer of ferritin, to below 5% [6]. We use 2.0% (w/v) $CdSO_4$ as a precipitant, and 0.2 M sodium acetate

buffer ($NaCH_3COO$) to fix pH at 5.05. The temperature of the solution in the growth cell is stabilized to 23 ± 0.01°C by a thermoelectric (Peltier) cooler [7]. The supersaturation is calculated as $\sigma = \ln(C/C_e)$, where C is concentration of the solution, C_e = 35 μg/mL [8] is solubility.

We used a phase-shifting interferometry technique specifically developed for this study [7]. The phase-shifting algorithm chosen by us employs five-image sequences captured with a phase shift of $\pi/2$; digital processing of the sequence allows reconstruction of the surface morphology with a depth resolution of 5 nm across a field of view of 1 × 1 mm^2, for details see ref [7]. The time traces of the normal growth rate R, local slope proportional to step density p, and step velocity v are recorded at select locations on the crystal surface with time resolution of 1 s [4].

Figure 1 shows the morphology of (111) faces of two ferritin crystals with sizes 200 μm and 470 μm. Figure 1a–e presents five interference images of the growing crystal surface recorded during 1 s with a phase shift of $\pi/2$ between them; the underlying assumption is that the surface does not change within this time period. Five images are combined to give one "phase-wrapped" image (Figure 1f, g) using, for each pixel

$$h = \frac{\lambda_{laser}}{2\pi n} \tan^{-1}\left[\frac{2(I_2 - I_4)}{2I_3 - I_5 - I_1}\right] \qquad (1)$$

where $I_1,\ldots,I_5$ are the intensity of a pixel in each of five images, h is the height on the respective point of crystal surface, λ_{laser} = 0.6328 μm is the laser wavelength and n = 1.3320 is the refractive index of the solution.

RESULTS AND DISCUSSION

Phenomenology of the time-dependent kinetics

During the growth of ferritin crystals the growth layers are always generated by 2D-nucleation. For small crystal sizes and $\sigma < 3$, the distribution of 2D-nuclei is uniform across the whole face and, on a macroscopic scale, the face remains flat as the crystal grows. For higher supersaturations and crystals larger than 100 μm, 2D-nucleition localizes at the facet edges and

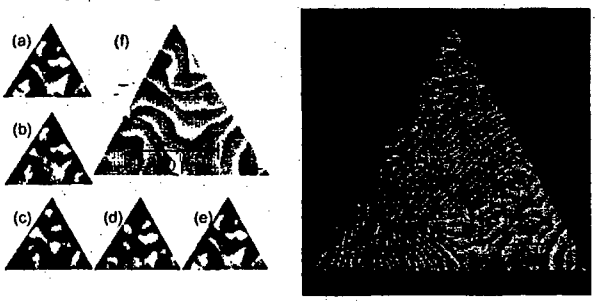

Figure 1. Typical morphology of a (111) face of a ferritin crystal. (a–e) A sequence of five interferometric images recorded with a phase shift of $\pi/2$. (f, g) The phase-wrapped images. The difference in height between the brightest and darkest pixels is $\lambda/4n$ = 0.119 μm. (f) σ = 4.0, (g) σ = 4.3. +, locations of layer generation; ×, locations of growth kinetics monitoring.

corners. Numerical modeling of diffusive-convective transport of crystallizing proteins has linked this localization to higher interfacial supersaturation at the edges [9].

Figures 2a–c show the time traces of the normal growth rate R, local slope p, and step velocity v recorded at the marked location near the facet center in Figure 1g at $\sigma = 4.3$. The R, p, v fluctuate by up to 100% of their respective average values. The fluctuations of local slope indicate that the unsteadiness occurs through the formation of step bunches. In order to analyze the fluctuations dependencies on different factors such as supersaturation, crystal size, location on the facet, we use Fourier decomposition of the three time traces. Earlier work has shown that the Fourier frequencies, characterizing the fluctuation time scales, and the Fourier amplitudes, corresponding to the deviations from average values of the respective kinetic variables, are reproducible characteristics of the unsteady behavior and only depend on the external conditions [10]. Figures 2d–f present the normalized Fourier spectra $A(f_m)/A_0$ of $R(t)$, $p(t)$ and $v(t)$.

Step-step interactions

Figures 2d–f show that the Fourier spectra for R, p, and v are similar. Since the Fourier spectra of p directly reflect the step bunching, we will use only these spectra in further considerations.

As shown in Figures 3a–c, the fluctuations are rather periodic. However, there appears to be no correlation between the fluctuations of the slope and the step velocity. The dependence of step velocity on local slope and the reduced concentration $(C - C_e)C_e^{-1}$ can be expressed as [10]

$$v = \frac{b_{step}(C - C_e)/C_e}{1 + kp} \qquad (2)$$

where b_{step} is an effective step kinetic coefficient and k is a parameter characterizing the step-step interactions. For non-interacting steps, $k = 0$; for strongly interacting steps such as those in lysozyme growth, where incorporation into steps is preceded by slow diffusion through the solution bulk and the terraces between the steps, k is in the range 1000–2000 [10]; for the growth of inorganic phosphates with a similar growth mechanism, values of k are ~1000 [11].

Prompted by the form of the $v(p)$ dependence in (2), we plot the reciprocal step velocity $1/v$ as a function of the local slope p for a trace recorded over several hours at the location near the center of facet in Figure 1g. To extract the deterministic link between v and p, we calculate the least square fit of the data to a straight line. From extrapolated intercept of this line with the

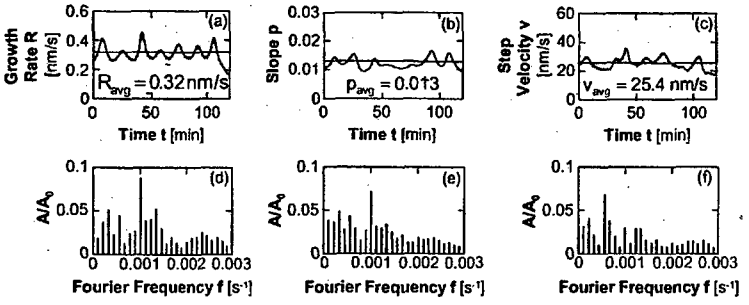

Figure 2. (a)–(c) Time traces of the normal growth rate R, the local slope p and the step velocity v recorded during growth of ferritin crystal at supersaturation $\sigma = 4.3$. (d)–(f) corresponding normalized Fourier spectra; in (d)–(f) $A/A_0 = 1$ at $f = 0$ is omitted.

ordinate axis and known value of $(C - C_e)/C_e = 71$, we obtain the value of $b_{step} = 4.8 \times 10^{-8}$ cm/s. The step kinetic coefficient $\beta = b_{step}/\Omega C_e = 11 \times 10^{-4}$ cm/s (Ω is the crystal volume per molecule, $\Omega C_e = 4.2 \times 10^{-5}$) is somewhat higher than the value of $\beta = 6 \times 10^{-4}$ cm/s obtained using AFM [8]. From the slope of the fit we calculate $k = 32$ and $kp_{avg} \approx 0.35$. This low value of k indicates a very weak interaction between steps, i.e. the diffusion supply fields around the steps do not overlap. This makes the ferritin system quite different from lysozyme, which is characterized by strong interaction between steps, which results in dependence of step velocity on slope [10].

Variations of the fluctuation patterns with the external conditions

Figure 3 presents the Fourier spectra of slope traces recorded at two locations on the facet shown in Figure 1g. Comparison of the spectra shows that the fluctuation amplitudes decrease as supersaturation increases and are greater near the facet edges than at the facet center. Note that the lower fluctuations at the facet center and at the higher supersaturations occur despite being accompanied by higher average vicinal slope. This is a remarkable observation, because the average vicinal slope has been identified as a major *destabilizing* factor for equidistant step trains [12]. We conclude that the mechanism leading to decay of the fluctuations is sufficiently strong to overpower the average slope effects.

We calculated the Fourier spectra of slope traces recorded at the center of two facets with different size (Figures 1f and 1g) at the same supersaturation. The maximum amplitude value is significantly higher for the smaller crystal, while the averaged slope is lower in this case.

We also compared the Fourier spectra of slope traces recorded simultaneously at two different locations of the facet shown in Figure 1f. The first location is close to the location of layer generation near the facet corner, while the second is further removed from the layer source. The amplitude of the slope fluctuations increases with the distance from layer source, while, as above, the averaged value of the slope decreases.

To understand these observations, we use that the crystal size, the location on the facet and the supersaturation are parameters that strongly affect the solute supply to the interface. Hence, the observed dependencies of the fluctuation amplitudes with these parameters indicate that, similar to lysozyme [3], the growth instability is due to the coupling of the nonlinear interfacial processes of growth to the bulk transport in the solution.

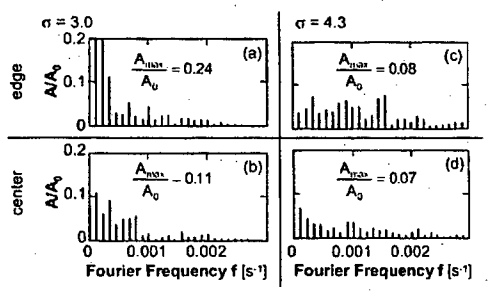

Figure 3. Fourier spectra of traces of the local slope p for the crystal of a 470 μm size shown in Figure 1g. (a) $\sigma = 3.0$, monitoring location at the facet edge, $p_{avg} = 0.006$; (b) $\sigma = 3.0$, monitoring location near the facet center, $p_{avg} = 0.008$; (c) $\sigma = 4.3$, edge, $p_{avg} = 0.012$; (d) $\sigma = 4.3$, center, $p_{avg} = 0.014$.

However, in all of the cases, the dependence of the fluctuation amplitudes on the respective parameter is opposite to that for lysozyme, and may appear counterintuitive. Thus, we would expect the faster growth at higher supersaturations to be more instable and with stronger fluctuations, we would expect the instabilities to evolve as the steps propagate down their pathway, and so on. This last controversy provides the key to understanding the unsteady behavior of the step trains in ferritin growth. Indeed, if the fluctuation amplitudes are dampened as the steps move on, it follows that the stable state, towards which the step train is converging, is the equidistant step train. Along this line of thought, we must conclude that the step bunches are generated at the location of step generation, i.e., the 2D nucleation process is highly unsteady, and consist of spurts of nucleated layers, leading to stacks of steps, followed by lower activity. The dependence of the fluctuation amplitudes on the supersaturation in the solution bulk suggests that the unsteady layer generation is caused by its coupling to the solute supply to the location of step generation.

The non-uniform step generation at the facet edges produces the step bunches. As the steps move away from their sources towards the facet center, the step bunches decay. An important factor for this decay is the lack of step-step interactions—such interactions are known to strongly destabilize the uniform step trains, and lead to increasing fluctuations [10].

The motion of steps and the evolution of the step bunches formed at the stage of layer generation is only affected by the coupled bulk transport and surface kinetics. The estimation of the kinetic Peclet number $Pe_k = \beta p \delta D$ (δ is the characteristic diffusion layer thickness, typically of the order of 200 μm, and $D = 3.2 \times 10^{-7}$ cm^2/s is diffusivity) gives value ~1.0. Hence, ferritin growth is predominantly controlled by the transport in the solution. For such systems, the rationale predicts higher stability at *even higher* relative weight of transport. Thus, we should expect lower kinetic fluctuations at higher supersaturations, at larger crystals sizes, and at the facet centers.

Spatial-temporal characteristics of the step patterns

The phase-shifting technique allows reconstruction of the surface morphology. Figure 4a shows the height profile along the line depicted in Figure 1g. The height decreases as the distance from layer sources increases. The corresponding slope profile and its spatial Fourier spectrum are shown in Figure 4b and c, respectively. The wave numbers in Figure 4c are reciprocal to the corresponding step bunch wavelengths λ. The maximum amplitude occurs at a wave number of 0.045 μm^{-1} corresponding to fluctuations with $\lambda_{max} \sim 21$ μm. From the time

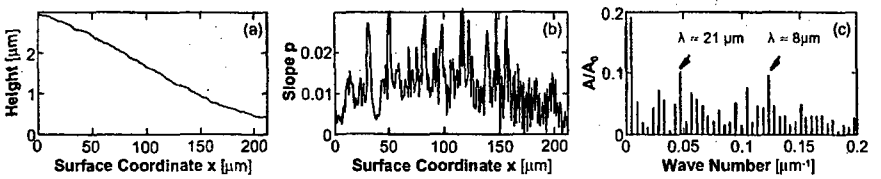

Figure 4. (a) Height and (b) local slope profiles along the line shown in Figure 1g. (c) Corresponding Fourier spectrum of p. The characteristic step bunch wavelengths λ are indicated in the plot. The first amplitude in (c) corresponds to the overall bending of the surface seen in (b)

traces measured at the location on profile line at the same $\sigma = 4.3$, see Figure 3c, we determine the characteristic step bunch frequency $f_{max} = 0.0016\ s^{-1}$ ($\Delta t \sim 10.7$ min). From these two values, we can evaluate the step bunch velocity as $v_{bunch} \approx \lambda_{max} f_{max} \sim 33$ nm/s. The value of v_{bunch} is close to mean step velocity under those conditions, $v \approx 35$ nm/s. Thus, in the case of non-interacting steps, the step bunches move with the same velocity as elementary steps.

CONCLUSIONS

Under steady growth conditions, ferritin growth kinetics fluctuate up to 100% of the average. The fluctuations reflect the dynamics of formation and evolution of step patterns. The lack of correlation of the step velocity and local slope indicates very weak step-step interactions. Correspondingly, the propagation rate of step bunches is same as elementary step velocity.

The unsteady growth is the result of the coupling between solute transport towards the interface and the nonlinear interfacial kinetics. The main factor introducing non-linearity onto the interfacial kinetics is the generation of layers via a 2D nucleation mechanism. The fluctuation amplitude decreases with increasing distance from the layer sources. Hence, for non-interacting steps growing under diffusion control the randomly arising step bunches decay and the stable growth mode is that via equidistant step trains.

These findings in a transport-controlled system provide a strong support to the rationale for the control of the step bunching instabilities in layer growth system that was previously based on observation with a kinetically controlled system.

ACKNOWLEDGMENTS

We thank Bill Thomas for the analysis and purification of the protein solutions and Kai Chen for supplementary AFM determinations. Research support was generously provided by the Office of Biological and Physical Sciences, NASA under Grants NAG8 1857and NAG8-1354.

REFERENCES

1. A. A. Chernov, "Modern Crystallography III, Crystal Growth." Springer, Berlin, 1984.
2. E. Bauser, *in* "Handbook of Crystal Growth" (D. T. J. Hurle, ed.), Vol. 3b, p. 879. North Holland, Amsterdam, 1994.
3. P. G. Vekilov, J. I. D. Alexander, and F. Rosenberger; *Phys. Rev. E* **54**, 6650 (1996).
4. P. G. Vekilov, L. A. Monaco, and F. Rosenberger, *J. Cryst. Growth* **148**, 289 (1995).
5. H. Lin, P. G. Vekilov, and F. Rosenberger, *J. Cryst. Growth* **158**, 552 (1996).
6. B. R. Thomas, D. Carter, and F. Rosenberger, *J. Cryst. Growth* **187**, 499 (1998).
7. O. Gliko, N. A. Booth, and P. G. Vekilov, *Crystal Growth and Design*, in press (2002).
8. K. Chen, unpublished.
9. H. Lin, F. Rosenberger, J. I. D. Alexander, and A. Nadarajah, *J. Cryst. Growth* **151**, 153 (1995).
10. P. G. Vekilov, B. R. Thomas, and F. Rosenberger, *J. Phys. Chem.* **102**, 5208 (1998).
11. N. A. Booth, A. A. Chernov, and P. G. Vekilov, *J. Cryst. Growth*, in print (2002).
12. A. A. Chernov, S. R. Coriell, and B. T. Murray, *J. Cryst. Growth* **132**, 405 (1993).